Optimal operation of smart multi-energy hub systems incorporating energy hub coordination and demand response strategy

O. Dzobo[a] and X. Xia[a]
Center for New Energy Systems, Department of Electrical, Electronic and Computer Engineering, University of Pretoria, Pretoria, South Africa

(Received 22 November 2016; accepted 25 June 2017; published online 13 July 2017)

This paper presents the operation and optimisation of a smart multi-energy hub system network using the energy hub concept. The case study system network includes integrated solar photovoltaic and thermal power generation units and natural gas combined heat and power unit systems. A demand response-dynamic economic emission optimisation model is applied in the case study and allows for a comparison of energy hub control strategies including the evaluation of economic and environmental criteria and power import between energy hubs. The results show a significant reduction of more than 50% in both the total generation cost and amount of emission when different energy hub control strategies are employed. The results also show that load shifting capabilities of different energy hub loads cannot be ignored as they reduce the electricity bill of energy hub customers. *Published by AIP Publishing.* [http://dx.doi.org/10.1063/1.4993046]

I. INTRODUCTION

The continuous growth in energy demand, dependency on fossil fuels, integration of distributed generation units, and the desire for sustainable and environmentally friendly energy sources have changed the state of the current power delivery grid and presented future challenges associated with planning and operation criteria of the power system network.[1,2] Many researchers have been re-oriented to model this new decision making environment and to propose new power system management frameworks in order to optimally control the interaction between these aspects.[3] Several techniques have been proposed in the literature for solving energy system networks with a mix of energy sources.[4,5] For example, at ETH Zurich, through their project titled, "Vision of Future Networks," a framework termed "Energy Hub concept" was proposed to solve such a kind of energy systems.[6] Recent research studies have started to address the integrated control of energy hub systems.[7] However, as the number of energy hub systems that are geographically dispersed starts to increase, it is expected that they will soon be connected to the conventional power system network in the near future. From this belief, it is therefore important to develop reliable and cost effective operational models of the interconnected energy hub systems to properly dispatch their different input energy carriers, which are characterised by different constraints.

The expansion of natural gas networks and their use in Combined Heat and Power (CHP) technologies has gained a high level of popularity in many developed countries.[1,8,9] Recently, the discovery of natural gas in Mozambique[10] has led the South African government to propose the construction of a natural gas pipeline network between the two countries.[11] The use of natural gas in CHP technologies to simultaneously generate heat and power in some industrial, large institutional facilities or other commercial facilities in South Africa is therefore expected to increase in the near future. Hence, this research paper considers a typical energy hub system

[a]Authors to whom correspondence should be addressed: odzobo@yahoo.com and xxia@up.ac.za

network with three energy hubs containing CHP generation units and solar photovoltaic (PV) power generation units as a case study.

A relevant number of recent research studies have dealt with characterisation and optimization of decentralised multi-energy systems.[4,7,12–14] The characterisation and optimization mathematical modelling focus mainly on providing an optimal choice of energy hub components, interactions between energy hubs, and other energy infrastructures; and purchase of optimal energy carriers and storage utilization. As more decentralised energy hub systems become geographically dispersed, the coordination of these energy hubs has become very important. The coordination between the energy hubs can be categorized as centralized and distributed.[5,15] In a centralized coordination of energy hub systems, the overall optimization problem is solved at each decision step using all parameters measured by the central supervisory controller. Figure 1(a) shows the centralized control architecture with three interconnected energy hubs and a central supervisory controller. The distributed coordination of energy hubs is achieved when each energy hub has its own respective distributed supervisory controller as shown in Fig. 1(b). The optimization problem is solved by iteratively solving the subproblems of each respective distributed supervisory controller within a set of rules. Each distributed supervisory controller has to coordinate its actions among neighbouring energy hubs in order to optimize the entire system network and guarantee continuous energy supply.

In most research studies in the literature, the optimization mathematical models of energy hubs are separated from the energy hub load.[16–19] The optimization models can be categorized as deterministic and stochastic models.[20] More complex optimization models of multi-energy hub systems such as deterministic model predictive control (MPC) techniques are also used for solving the optimization problems of interconnected energy hub systems.[15,20] The main disadvantage of these proposed methods has been that the interconnected load is decoupled from the operations of the interconnected energy hub system. Due to the decoupling, there is underutilization of the load shifting opportunities of the interconnected load in the energy hub system network. This may lead to suboptimal operation solutions of the interconnected energy hub system. Several other authors have addressed demand response (DR) strategies combined with energy hub system optimisation in short-term and multi-period optimization models. Reference 21 introduced the energy hub concept with the stochastic demand response using the model predictive control (MPC). The demand response load model for the connected energy hub customers is lumped together and is taken as a stochastic variable. Centralised and distributed control

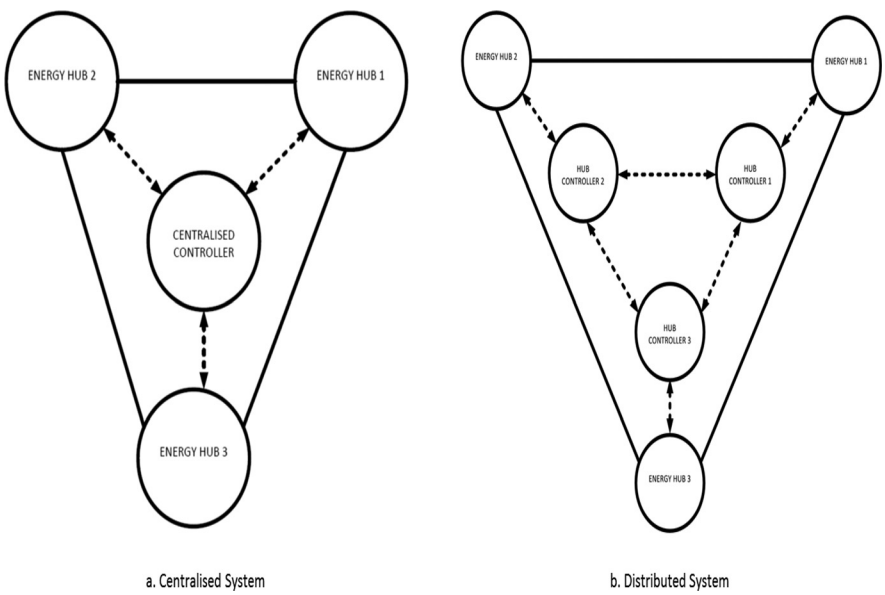

FIG. 1. Different control architectures for interconnected energy hubs.

schemes of the energy hub systems were considered in the analyses. In Ref. 22, the mathematical optimization formulation described has all the input energy hub load data specified at fixed times using deterministic values. However, these analyses have the disadvantage that different energy hub loads operate at different times during the day, and it is difficult to see the actual allocation of time for the individual energy hub loads. In some cases, the energy hub loads are power shiftable and/or sequentially time shiftable, which may not be taken into account in the analysis. Therefore, the use of stochastic optimal energy hub loads or non-shiftable deterministic energy hub loads might not reflect the best times of operation for the individual energy hub loads. In this paper, individual energy hub loads for three different energy hub customers are considered. In addition, sequential time-shiftable and power shiftable energy hub loads are considered in the analyses. A combined demand response-dynamic economic emission dispatch (DR-DEED) strategy for future power system networks in the context of multi-energy hub systems is presented. Both centralised and distributed control strategies are used for the coordination of the energy hubs. The objective of the combined DR-DEED strategy is to maximize the economic benefit of both electricity customers and power utility by reducing their electricity bill/cost and reducing the generation cost and amount of emission of the thermal power generation units.

The contribution of the current paper can be summarized as follows:

- A multi-energy system network with three energy hubs is considered as a case study. Each energy hub has a mix of energy systems, i.e., thermal power generation units, CHP units, and solar PV power generation units.
- A demand response program for the connected energy hub loads is proposed, with sequential time-shiftable and power shiftable loads considered.
- The CHP units considered in this paper have a non-convex feasible operation region (FOR) and are modelled using a mixed-integer linear programming technique. The ramp rates of both thermal power generation units and CHP units are also considered in the analysis.
- Two control strategies are used for the coordination of the energy hubs, i.e., centralised and distributed control strategies.

II. ENERGY HUB CONCEPT

Figure 2 shows an example of an energy hub system. The energy hub output port provides electricity, heating, and cooling to the energy hub customer loads. Both converters and storage devices are incorporated into the energy hub system. The converters, e.g., electric transformer, CHP device, and furnace, are used to change input carrier energy into another form of energy. In some cases, direct connections between the energy hub input and output ports are used when there is no change in the input energy. For example, electric cables and/or overhead lines can be used to transport electricity to the energy hub output port. For the storage of excess energies such as power or heat, storage devices are incorporated into the energy hub system. For example, batteries are used for the storage of electric energy and/or steam boilers for conserving heat energy. Figure 3(a) shows a converter with one input and one output such as a transformer. At any given time, t, the input power $P_{\theta,t}$ and output power $L_{\phi,t}$ are coupled as follows:

$$L_{\phi,t} = C_{\theta\phi} * P_{\theta,t}, \tag{1}$$

where $C_{\theta\phi}$ is the converter efficiency for the power conversion of the device. Similarly, the input and output parameters in Fig. 3(b) can be expressed as follows:

$$\begin{bmatrix} L_{\phi,t} \\ L_{\theta,t} \end{bmatrix} = \begin{bmatrix} C_{\theta\phi} \\ C_{\theta\theta} \end{bmatrix} P_{\theta,t}, \tag{2}$$

where $C_{\theta\phi}$ and $C_{\theta\theta}$ are the coupling factors for the respective converter's energy efficiencies. In the case where various energy carriers and converters make up the energy hub system, the

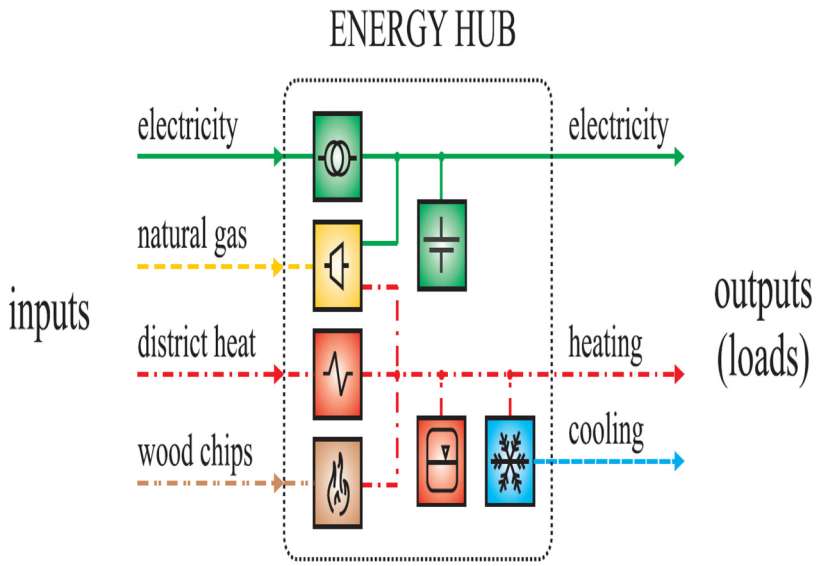

FIG. 2. Example of an energy hub.

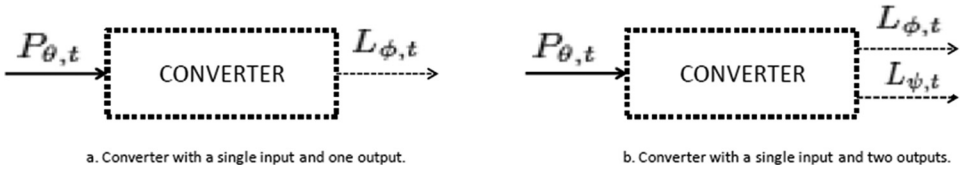

FIG. 3. Model of power converters with inputs and outputs.

general formulation of the multi-input multi-output (MIMO) energy hub system can be expressed as shown in the following:

$$\begin{bmatrix} L1_{\phi,t} \\ L2_{\theta,t} \\ . \\ . \\ . \\ Ln_{\omega,t} \end{bmatrix} = \begin{bmatrix} C1_{\phi\phi} & C1_{\theta\phi} & . & . & . & C1_{\omega\phi} \\ C2_{\phi\theta} & C2_{\theta\theta} & . & . & . & C2_{\omega\theta} \\ . & . & . & . & . & . \\ . & . & . & . & . & . \\ . & . & . & . & . & . \\ Cn_{\phi\omega} & Cn_{\theta\omega} & . & . & . & Cn_{\omega\omega} \end{bmatrix} \begin{bmatrix} P_{\phi,t} \\ P_{\theta,t} \\ . \\ . \\ . \\ P_{\omega,t} \end{bmatrix}. \tag{3}$$

III. CASE STUDY

Figure 4 shows the interconnected energy hub system network consisting of three energy hub systems that are interconnected. It has two interconnected networks of natural gas and electricity. The natural gas network consists of two network nodes, and the electricity network has three network nodes. This case study represents a typical urban energy supply network divided into three supply areas: residential load (hub 1), commercial load (hub 2), and industrial load (hub 3). Each energy hub has a different internal structure which is dependent on the type of loads present at the respective energy hub.

Each energy hub has its own local electrical energy production G_{pvi} and G_{ei} and heat production G_{ngi} for $i \in 1, 2, \ldots, n$. Energy hubs 2 and 3 consume electric power G_{ei} and natural gas G_{ngi} and supplies energy to their electric load L_{ek} and heat load L_{hk} for $k \in 1, 2, \ldots, K$. Energy hub 1 has only electric load L_{ek} and is supplied by solar PV power generation G_{pvi} and thermal power generation G_{ei}. Tables I and II show the converter efficiency data, and thermal power generation and CHP generation unit data, respectively, for the multi-energy hub system

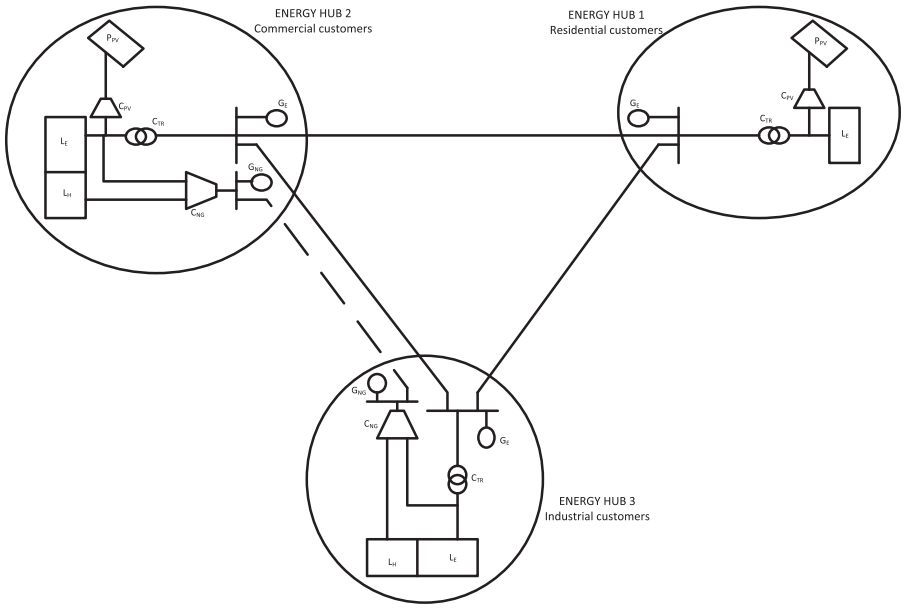

FIG. 4. Single-line diagram of the smart multi-energy hub system network.

TABLE I. Converter efficiency data of the multi-energy hub system network.

Converter efficiency (%)						
Solar PV		Transformer			Natural gas	
C_{PV1}	C_{PV2}	C_{TR1}	C_{TR2}	C_{TR3}	C_{NG2}	C_{NG3}
0.95	0.95	0.98	0.98	0.98	0.96	0.96

network. The time of use (TOU) electricity prices and heat demand for the energy hub customers are presented in Tables III and IV, respectively. Aggregate energy hub loads for residential, commercial, and industrial customers connected at different energy hubs are presented in Tables V, VI, and VII, respectively.

TABLE II. Thermal generation unit data of the multi-energy hub system network.

Hub No.	Gen. No.	$P_i^{\max}$ MW	$P_i^{\min}$ MW	a_i \$/h	b_i \$/MWh	c_i \$/MW^{2}h	d_i lb/h	e_i lb/MWh	f_i lb MW^{2}h	UR_i MW/h	DR_i MW/h
Hub 1	1	500	100	200	38.5397	0.007	13.8593	0.32767	0.00419	80	120
	2	200	50	1450.7045	38.2704	0.0095	330.0056	0.32767	0.00419	50	90
	3	300	80	1450.7045	38.3055	0.009	330.0056	−0.54551	0.00683	65	100
Hub 2	1	340	73	1469.4026	40.3965	0.03280	360.0012	0.32767	0.00419	80	80
	2	300	63	200	11.0	0.00354	38.3055	−0.51116	0.00461	50	50
	3	130	20	220	36.5104	0.0121	42.8955	−0.51116	0.00461	30	30
	4	55	10	200	40.5407	00.1295	40.2669	−0.51116	0.00683	30	30
	CHP 1	247	98.8	220	10.5	0.00345	…	…	…	70	70
Hub 3	1	500	100	190	38.5397	0.007	42.8955	0.32767	0.00419	80	120
	2	200	50	1455.6056	38.2704	0.0095	350.0056	0.32767	0.00419	50	90
	3	470	135	220	38.5397	0.009	40.2669	−0.54551	0.00683	80	80
	4	160	57	240	39.5804	0.0179	13.8593	−0.51116	0.00461	50	50
	CHP 2	125.8	45.1	240	…	0.0265	13.8593	…	…	50	50

TABLE III. TOU electricity prices of the multi-energy hub system network for 24 h.

Time (t)	1	2	3	4	5	6	7	8	9	10	11	12
Residential TOU price	0.4088	0.4088	0.4088	0.4088	0.4088	0.6413	0.6413	0.9293	0.9293	0.9293	0.6413	0.6413
Commercial TOU price	0.3979	0.3979	0.3979	0.3979	0.3979	0.6272	0.6272	0.9112	0.9112	0.9112	0.6272	0.6272
Industrial TOU price	0.3853	0.3853	0.3853	0.3853	0.3853	0.6073	0.6073	0.8825	0.8825	0.8825	0.6073	0.6073
Time (t)	13	14	15	16	17	18	19	20	21	22	23	24
Residential TOU price	0.6413	0.6413	0.6413	0.6413	0.6413	0.6413	0.9293	0.9293	0.6413	0.6413	0.4088	0.4088
Commercial TOU price	0.6272	0.6272	0.6272	0.6272	0.6272	0.6272	0.9112	0.9112	0.6272	0.6272	0.3979	0.3979
Industrial TOU price	0.6073	0.6073	0.6073	0.6073	0.6073	0.6073	0.8825	0.8825	0.6073	0.6073	0.3853	0.3853

TABLE IV. Heat demand for different energy hubs for 24 h.

Time (t)	1	2	3	4	5	6	7	8	9	10	11	12	13	14	15	16	17	18	19	20	21	22	23	24
Hub 2	165	152	163	140	145	173	109	133	136	160	111	145	190	151	163	150	121	121	69	132	123	84	75	100
Hub 3	125	102	103	130	135	63	89	102	112	115	120	123	119	125	126	125	122	120	115	109	102	84	75	60

TABLE V. Aggregate residential customer loads.

Type of load	E_{DAILY} (MWh)	α_a (h)	β_a (h)	Z_a (h)
Inflexible				
Load 1	300	1	24	24
Load 2	100	12	16	5
		20	22	3
Flexible				
Load 3	Hourly consumption: 0–50 Daily requirement: 200	1	24	…
Load 4	Hourly consumption: 0–150 Daily requirement: 550	21	9	…
Load 5	Hourly consumption: 0–100 Daily requirement: 400	20	8	…
Load 6	50	8	20	3
Load 7	150	16	22	4

A. Energy hub system component modelling

1. CHP unit modelling

The CHP units considered in this paper have an interdependent relationship between their respective heat and power outputs. Each CHP unit operates within a feasible operation region (FOR). Figures 5 and 6 show the type of CHP units considered in this paper and their respective feasible operation regions. In Fig. 5, the CHP unit is constrained by three operational parameters, namely, maximum power generation (AB), minimum power generation (BCD), and maximum heat generation (B). The FOR of the CHP unit shows that as the heat generation of the CHP unit increases, its corresponding power generation decreases along the boundary curve AB. However, along the boundary curve BC, the power generation and heat generation of the CHP unit decrease concurrently. Equations (4)–(8) are used to define the FOR of the CHP unit

TABLE VI. Aggregate commercial customer loads.

Type of load	E_{DAILY} (MWh)	α_a (h)	β_a (h)	Z_a (h)
Inflexible				
Load 1	400	1	24	24
Load 2	80	12	16	3
	80	15	17	3
Load 3	110	10	14	5
	50	16	20	5
Load 4	50	8	8	1
	150	12	12	1
Flexible				
Load 5	Hourly consumption: 0–300	8	20	…
	Daily requirement: 800			
Load 6	Hourly consumption: 20–50	01	6	…
	50–100	21	24	…
	Daily requirement: 350			
Load 7	50	8	20	3
Night-time				
Load 8	150	21	03	4

$$P_{i,t} - P_{i,A} - \frac{P_{i,A} - P_{i,B}}{H_{i,A} - H_{i,B}}(H_{i,t} - H_{i,A}) \leq 0$$
$$\Rightarrow P_{i,t} + \frac{8}{45}H_{i,t} - 247 \leq 0, \tag{4}$$

$$P_{i,t} - P_{i,B} - \frac{P_{i,B} - P_{i,C}}{H_{i,B} - H_{i,C}}(H_{i,t} - H_{i,B}) \leq 0$$
$$\Rightarrow P_{i,t} - \frac{134}{75.2}H_{i,t} + 105.74468 \leq 0, \tag{5}$$

TABLE VII. Aggregate industrial customer loads.

Type of load	E_{DAILY} (MWh)	α_a (h)	β_a (h)	Z_a (h)
Inflexible				
Load 1	500	1	24	24
Load 2	100	10	17	8
	70	18	20	3
Flexible				
Load 3	Hourly consumption: 50–100	7	16	…
	Daily requirement: 300			
Load 4	150	9	20	6
Night-time				
Load 5	50	21	24	5
		01	06	6
Load 6	150	22	3	6
Load 7	Hourly consumption: 100–250	21	6	…
	Daily requirement: 700			
Load 8	1st hour: 100	21	6	…
	6th hour: 50			

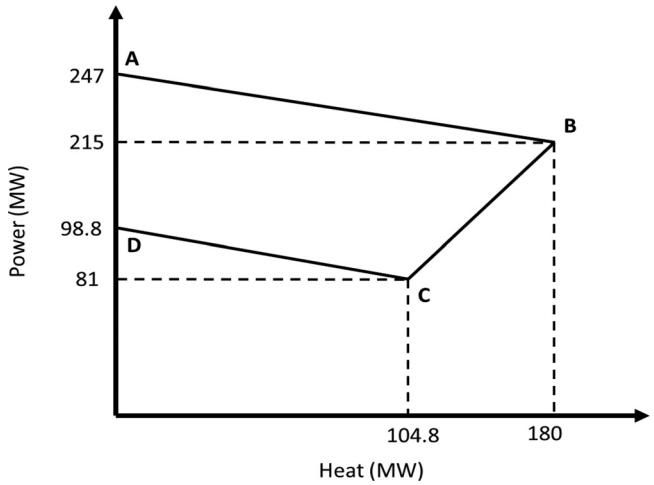

FIG. 5. FOR of a CHP unit at hub 2.

$$P_{i,t} - P_{i,C} - \frac{P_{i,C} - P_{i,D}}{H_{i,C} - H_{i,D}}(H_{i,t} - H_{i,C}) \leq 0$$

$$\Rightarrow P_{i,t} + \frac{17.8}{104.8} H_{i,t} - 98.8 \leq 0, \tag{6}$$

$$0 \leq H_{i,t} \leq 180, \tag{7}$$

$$0 \leq P_{i,t} \leq 247, \tag{8}$$

where the FOR parameter points of the CHP unit are represented by indices A, B, C, and D. Equation (4) represents the area under the boundary curve AB, while Eqs. (5) and (6) define the areas above the boundary curves BC and CD, respectively. When the CHP unit is not operating, its power generation and heat generation are set to zero using Eq. (7), and during operation, it is restricted to operate above the maximum power generation and heat generation using Eq. (8). The CHP unit has ramp rates during start and shut down times of its operation. Equation (9) presents a constraint to ensure that the CHP unit ramp rate limits are not violated

$$-DR_i^{CHP} \leq P_{i,t+1}^{CHP} - P_{i,t}^{CHP} \leq UR_i^{CHP}, \tag{9}$$

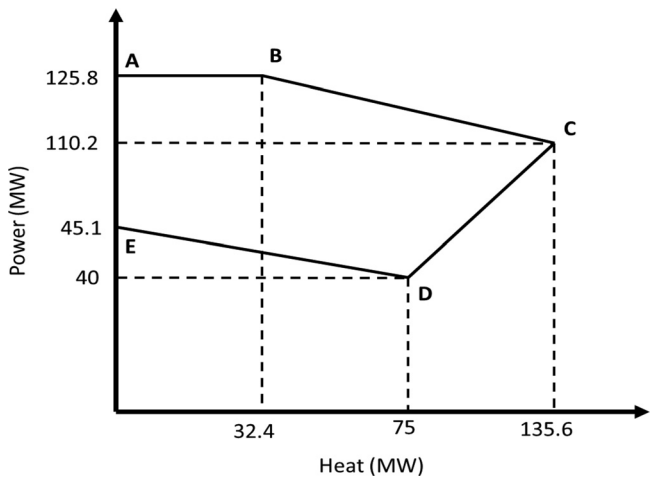

FIG. 6. FOR of a CHP unit at hub 3.

where DR_i^{CHP} and UR_i^{CHP} are the maximum ramp down rates and maximum ramp up rates of the i^{th} CHP unit, respectively.

Figure 6 shows the FOR of the CHP unit connected at hub 3 which is defined by the boundary curve ABCDE. Similarly, it is constrained by the same three operational parameters as the CHP unit connected at hub 2 (see Fig. 5). Heat generation increases along the boundary curve BC as the corresponding power generation of the CHP unit decreases. However, along the boundary curve CD, heat generation and power generation decrease concurrently. The FOR of the CHP unit is defined by the following equations:

$$P_{i,t} - P_{i,B} - \frac{P_{i,B} - P_{i,C}}{H_{i,B} - H_{i,C}}(H_{i,t} - H_{i,B}) \leq 0$$
$$\Rightarrow P_{i,t} - \frac{15.6}{103.2}H_{i,t} - 130.69767 \leq 0, \tag{10}$$

$$P_{i,t} - P_{i,C} - \frac{P_{i,C} - P_{i,D}}{H_{i,C} - H_{i,D}}(H_{i,t} - H_{i,C}) \leq 0$$
$$\Rightarrow P_{i,t} - \frac{5.1}{75}H_{i,t} - 45.1 \leq 0, \tag{11}$$

$$P_{i,t} - P_{i,D} - \frac{P_{i,D} - P_{i,E}}{H_{i,D} - H_{i,E}}(H_{i,t} - H_{i,D}) \leq 0$$
$$\Rightarrow P_{i,t} - \frac{70.2}{60.6}H_{i,t} - 46.881188 \leq 0, \tag{12}$$

$$0 \leq H_{i,t} \leq 135.6, \tag{13}$$

$$0 \leq P_{i,t} \leq 125.8, \tag{14}$$

where the FOR parameter points of the CHP unit are represented by indices A, B, C, D, and E. Equation (10) represents the area under the boundary curve BC, while Eqs. (11) and (12) define the areas above the boundary curves DE and CD, respectively. When the CHP unit is not operating, its power generation and heat generation are set to zero using Eq. (13), and during operation, it is restricted to operate above maximum power and heat generation using Eq. (14). The CHP unit has ramp rates during start and shut down times of its operation. Equation (15) presents a constraint to ensure that the CHP unit ramp rate limits are not violated

$$-DR_i \leq P_{i,t+1} - P_{i,t} \leq UR_i, \tag{15}$$

where DR_i and UR_i are maximum ramp down rates and maximum ramp up rates of the ith CHP unit, respectively.

In this paper, a CHP unit is modelled to have a convex cost function in both power and heat generation.[14,23] The quadratic function approximation is the most commonly used function for modelling the cost function, and it is said to be a more accurate function than others.[23,24] Hence, in this paper, the form of the fuel cost function of CHP units adopted is given as follows:

$$C_i^{CHP}\left(P_{i,t}^{CHP}, H_{i,t}^{CHP}\right) = a_i + b_i P_{i,t}^{CHP} + c_i\left(P_{i,t}^{CHP}\right)^2 + d_i H_{i,t}^{CHP} + e_i\left(H_{i,t}^{CHP}\right)^2 + f_i\left(P_{i,t}^{CHP}, H_{i,t}^{CHP}\right). \tag{16}$$

2. Convectional thermal power generation unit modelling

The generation cost function of thermal power generation units has been derived using the linear cost function, piecewise linear cost function, quadratic cost function, etc.[24] Using the same reasoning applied to the CHP units, the quadratic fuel cost function of the power generation unit is adopted. The generation cost function for thermal power generation units is defined in terms of its output power. The fuel cost function of the power generation unit is defined as follows:

$$C_i^G(P_{i,t}) = a_i + b_i P_{i,t}^G + c_i \left(P_{i,t}^G\right)^2. \tag{17}$$

As thermal power generation units burnt the fuel for their power output, there are a lot of emissions as a result of such operation. The emission function of the thermal power generation units is expressed in terms of the sum of all types of emissions; common examples are NO, SO_2, and CO_2. In this paper, the emission functions for NO, SO_2, and CO_2 are taken as quadratic functions and are expressed as follows:

$$E_i(P_{i,t}) = g_i + h_i P_{i,t} + m_i P_{i,t}^2. \tag{18}$$

The thermal power generation unit operation constraints ensure that the thermal power generation unit's power output limits are not exceeded, i.e.,

$$P_i^{min} \leq P_i \leq P_i^{max}, \tag{19}$$

where P_i^{min} and P_i^{max} are lower and upper bounds for power outputs of the ith thermal power generation unit, respectively. The thermal power generation units have ramp rates during start and shut down times of their operation. Equation (20) presents a constraint to ensure that the thermal power generation unit ramp rate limits are not violated.

$$-DR_i \leq P_{i,t+1} - P_{i,t} \leq UR_i, \tag{20}$$

where DR_i and UR_i are maximum ramp down rates and maximum ramp up rates of the ith thermal power generation unit, respectively.

3. Demand response load modelling

The energy hub customers are assumed to have the same behaviour in terms of the varying load response to the electricity price variation. The electricity price information is released a day ahead, and the energy hub supervisory controller arranges the operation of energy hub loads for the next 24 h. The scheduling horizon and the resolution of the scheduling horizon are assumed to be 24 h and 1 h, respectively. The DR objective function minimizes the electricity bill of the energy hub customers without affecting their daily energy requirements. Let $\mathbf{A}$ denote the set of energy hub load demand, and then $L_a^t \geq 0$ is the load demand by energy hub load $a \in \mathbf{A}$ at time t. The total daily energy requirement from energy hub load a over one day can be defined as follows:

$$\mathbf{E}_{\mathbf{DAILY,a}} = \sum_{t=1}^{T} L_a^t. \tag{21}$$

For inflexible energy hub load which cannot be shifted to any time slot, the total energy requirement for the whole operation period of the energy hub load is given by

$$\sum_{t=\alpha_a}^{\beta_a} L_a^t = E_a \quad \forall a \in \mathbf{A}, \tag{22}$$

where E_a is the total energy requirement for the whole operation of the energy hub load, α_a is the beginning of acceptable operation time, and β_a is the end of acceptable operation time. Equation (22) ensures that the operation period of the energy hub load is finished before the deadline and is equal to the total energy requirement of operation. It is also required that $L_a^t = 0 \; \forall t < \alpha_a$ and $t > \beta_a$. For example, load 2 in Table V has two periods of operation, i.e., ($\alpha_1 = 12$, $\beta_1 = 16$) and ($\alpha_2 = 20$, $\beta_2 = 22$). The total daily energy requirement for load 2 is given as follows:

$$E_{DAILY,Load2} = \sum_{t=12}^{16} L_{Load2}^{t} + \sum_{t=20}^{22} L_{Load2}^{t}$$
$$= 500 + 300$$
$$= 800\text{MWh}.$$

It is also required that $L_{Load2}^{t} = 0 \,\forall\, 1 \leq t \leq 11$, $17 \leq t \leq 19$, and $23 \leq t \leq 24$.

In the case where the hourly energy hub load demand is known in terms of range of load levels, L_a^t is treated as a variable. For energy hub load $a \in \mathbf{A}$ which has a maximum hourly load level γ_a^{max} and a minimum hourly load level γ_a^{min}, the total daily energy requirement is given as follows:

$$\sum_{t=\alpha_a}^{\beta_a} L_a^t = E_{DAILY,a} \quad \forall\, a \in \mathbf{A} \;\; t \in [\alpha_a, \beta_a], \quad \gamma_a^{min} \leq L_a^t \leq \gamma_a^{max}. \tag{23}$$

For example, in load 3 in Table V, the energy hub load operates for the whole 24 h of the day, i.e., $\alpha = 1$, $\beta = 24$. The energy hub load can take any value between $\gamma_{Load3}^{min} = 0$ and $\gamma_{Load3}^{max} = 50\text{MWh}$ at each hour t. However, the total daily energy requirement for the energy hub load must be equal to 200 MWh.

Flexible energy hub loads can be arranged in several hours while ensuring that the total energy is supplied. Let $\mathbf{R}\,(\subset \mathbf{A})$ denote the set of indexes of the flexible energy hub load. For energy hub load $a \in \mathbf{R}$, if X_a denotes the fundamental load demand pattern as $\left(\varepsilon_a^1, \varepsilon_a^2, \ldots, \varepsilon_a^t, \ldots, \varepsilon_a^T\right)$ where $\varepsilon_a^t \geq 0$, the ath flexible energy hub load can have T possible patterns which are obtained by circular shifting the fundamental load demand pattern. In order to select one possible load demand pattern for optimization, a binary switching integer vector s_a is used. The binary switching integer vector s_a is defined as $s_a = \left(s_a^1, s_a^2, \ldots, s_a^t, \ldots, s_a^T\right)$, where $s_a^t \in (0, 1)$. The position of a binary integer one (1) means the starting time at which the energy hub load is switched ON. The binary switching integer vector therefore has only one non-zero element equal to one (1) in order to ensure that each energy hub load is switched only once per each operation. For energy hub load $a \in \mathbf{R}$, this constraint can be written as follows:

$$\sum_{t=1}^{T} s_a^t = 1. \tag{24}$$

By using s_a, the energy hub load demand scheduling plan L_a can be written as follows:

$$L_a = s_a * \mathrm{X}_a^{\mathbf{C}} \quad \forall a \in \mathbf{R}, \tag{25}$$

where the 24 × 24 matrix X_a^C column is the circulant matrix of the fundamental load demand pattern, X_a, i.e.,

$$\mathrm{X}_a^C = \begin{pmatrix} \varepsilon_a^1 & \varepsilon_a^{24} & . & . & . & . & \varepsilon_a^2 \\ \varepsilon_a^2 & \varepsilon_a^1 & . & . & . & . & \varepsilon_a^3 \\ . & . & . & . & . & . & . \\ . & . & . & . & . & . & . \\ . & . & . & . & . & . & . \\ \varepsilon_a^{24} & \varepsilon_a^{23} & . & . & . & . & \varepsilon_a^1 \end{pmatrix}.$$

For simplicity, let us take a 5 h load schedule for energy hub load a. If the fundamental load demand pattern is given as $X_a = [100\ 0\ 0\ 50\ 0]$, then

$$X_a^C = \begin{pmatrix} 100 & 0 & 50 & 0 & 0 \\ 0 & 100 & 0 & 50 & 0 \\ 0 & 0 & 100 & 0 & 50 \\ 50 & 0 & 0 & 100 & 0 \\ 0 & 50 & 0 & 0 & 100 \end{pmatrix}.$$

To choose one of the energy hub load demand patterns, a binary switching vector s_a is used. For example, to choose the first column, the first element of s_a is set to binary integer 1, i.e., $s_a = [1\,0\,0\,0\,0]$. The energy hub load demand pattern for optimisation is given as follows:

$$L_a^{\mathsf{T}} = X_a^C * s_a^{\mathsf{T}}, \tag{26}$$

$$= \begin{pmatrix} 100 & 0 & 50 & 0 & 0 \\ 0 & 100 & 0 & 50 & 0 \\ 0 & 0 & 100 & 0 & 50 \\ 50 & 0 & 0 & 100 & 0 \\ 0 & 50 & 0 & 0 & 100 \end{pmatrix} \begin{pmatrix} 1 \\ 0 \\ 0 \\ 0 \\ 0 \end{pmatrix}, \tag{27}$$

$$L_a = [100\ 0\ 0\ 50\ 0].$$

Similarly, to choose the second, third, fourth, and fifth columns of the circulant matrix X_a^C, the second, third, fourth, and fifth elements of s_a are set to binary integer 1, respectively. If ε_a^t is a variable and bounded by a minimum hourly load level $\gamma_a^{min} \geq 0$ and a maximum hourly load level γ_a^{max}, with a positive constant E_a denoting the total daily energy requirement limit for the ath energy hub load, the load demand scheduling plan L_a for the flexible energy hub load can be written as follows:

$$L_a^{\mathsf{T}} = \mathrm{X}_a^{\mathrm{C}} * s_a^{\mathsf{T}} \quad \forall \quad \sum_{t=\alpha}^{\beta} \varepsilon_a^t = \mathrm{E}_a, \quad \gamma_a^{min} \leq \varepsilon_a^t \leq \gamma_a^{max},\ a \in \mathbf{R}. \tag{28}$$

B. DR-DEED problem formulation

The first step in the DR-DEED optimization model is to solve the demand response (DR) objective function. The objective of the DR strategy is to minimize the electricity cost of energy hub customers. The output load profile from the DR objective function is used as an input to the dynamic economic emission dispatch (DEED) model. Given a specific period of operation for the thermal power generation units and CHP units, the DEED model is about simultaneously minimizing both the generation cost and the amount of emission and at the same time ensuring that the system network load demand and generation unit operation constraints are satisfied.

Assuming that the electricity pricing vectors for all the hours of the day are given as $\rho = (\rho_1, \rho_2, \ldots, \rho_{24})$, the electricity cost at each hour t, $t \in 1, 2, \ldots, T$, is given by

$$EH_{\cos t,t} = \rho_t * L_{ET,t}, \tag{29}$$

where $L_{ET,t} = L^t_{Efixed,a} + L^t_{Eflexible,a} + L^t_{Enighttime,a}$, i.e., sum of fixed, flexible, and night-time energy hub loads at any given time t. The general DR optimisation problem formulation for the whole day is given as follows:

$$DR_{min} = min\left[\sum_{t=1}^{T} \rho_t L_{ET,t}\right]. \tag{30}$$

Subject to: Flexible and non-flexible energy hub load constraints, i.e., Eqs. (21)–(28).

TABLE VIII. Possible combinations of communication between energy hub system networks.

Scenario	Possible combination
1	Distributed control scheme without communication
2	Centralised control scheme
3	Distributed control scheme with communication: $E1 \rightarrow E2 \rightarrow E3$
4	Distributed control scheme with communication: $E1 \rightarrow E3 \rightarrow E2$
5	Distributed control scheme with communication: $E2 \rightarrow E1 \rightarrow E3$
6	Distributed control scheme with communication: $E2 \rightarrow E3 \rightarrow E1$
7	Distributed control scheme with communication: $E3 \rightarrow E1 \rightarrow E2$
8	Distributed control scheme with communication: $E3 \rightarrow E2 \rightarrow E1$

The energy hub load demand $L_{ET,t}$ that minimizes the electricity cost for the whole day becomes the input to the DEED optimisation problem. In this stage, a weighting factor μ is introduced to transform the multi-objective optimization problem into a weighted single objective optimization problem. This would allow the contradicting power generation fuel cost objective and emission objective functions to be simultaneously minimized. The weighting factor, μ, blends the generation cost and amount of emission of the power generation units. The mathematical formulation of the weighted single objective optimization can be expressed as follows:

$$DR - DEED = min[\mu C_{cost} + (1-\mu) E_{cost} + DR_{min}]. \tag{31}$$

Subject to: (i) Power and heat demand balance constraints; (ii) CHP units and thermal power generation unit constraints, i.e., Eqs. (4)–(15), (19), and (20); and (iii) flexible and non-flexible energy hub load constraints, i.e., Eqs. (21)–(28),where

$$C_{cost} = C_i^G(P_{i,t}) + C_i^{CHP}\left(P_{i,t}^{CHP}, H_{i,t}^{CHP}\right)], \tag{32}$$

$$E_{cost} = E_i(P_{i,t}). \tag{33}$$

The power and heat demand balance constraints are dependent on the scenario being considered. These constraints are therefore explained in each scenario considered. In this analysis, two stages were involved. The first stage investigated the effect of the DR strategy on energy hub customers' electricity cost. Two scenarios were considered: (1) without the DR strategy and (2) with the DR strategy. In the second stage, the power import between energy hubs, generation cost, and the amount of emission were investigated for 8 different scenarios. Scenario 2 of the first stage was used in the second stage for all the scenarios considered. In the second stage, 8 scenarios were considered in the case study and are given in Table VIII.

The arrow shows the sequence of communication between the energy hubs.

C. Case 1: Effect of DR strategies

In the first scenario, i.e., without the DR strategy, flexible appliances are set to start at the beginning of their preference starting time. The electricity pricing vector of the respective energy hub customers is used in Eq. (30) to calculate their respective total electricity costs. In the case where the DR strategy is used, i.e., scenario 2, the DR optimization model of Eq. (30) is used to minimize the respective energy hub customers' total electricity cost. The total electricity cost minimization is achieved by changing the parameters on the power-shiftable and time-shiftable energy hub loads under their respective constraints. Table IX shows different total electricity costs for the energy hubs. It can be clearly seen that when the DR strategy is used, there is reduction in the electricity cost for the energy hub customers. This shows the significance of taking into account the load shifting capabilities of energy hub loads.

TABLE IX. Energy hub customer electricity cost for different DR strategies.

Energy hub	With DR strategy	Without DR strategy
1	5.5761×10^5	5.828×10^5
2	6.9376×10^5	6.9644×10^5
3	9.5403×10^5	9.6948×10^5

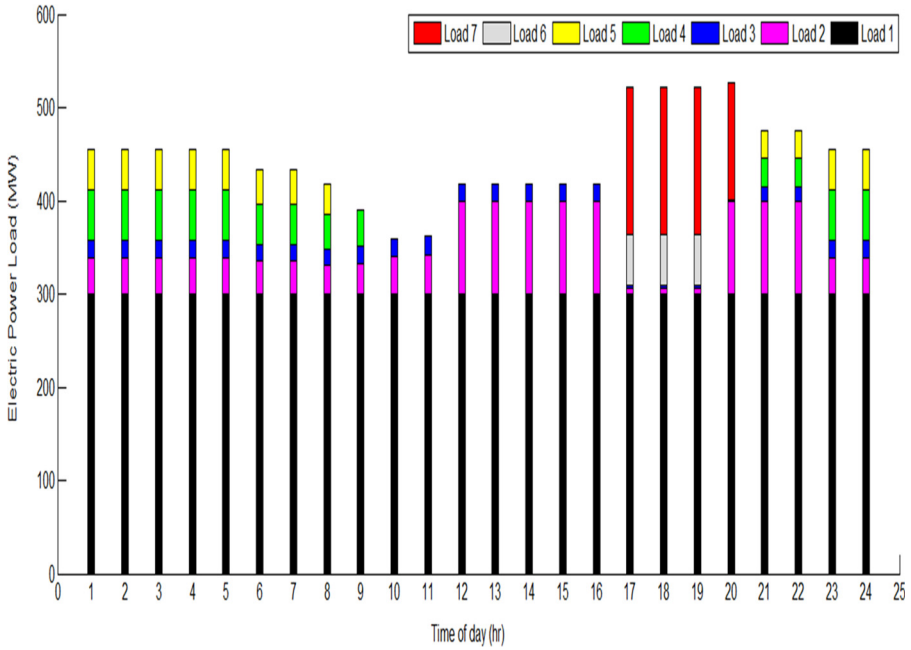

FIG. 7. Residential customers' optimal load for energy hub 1.

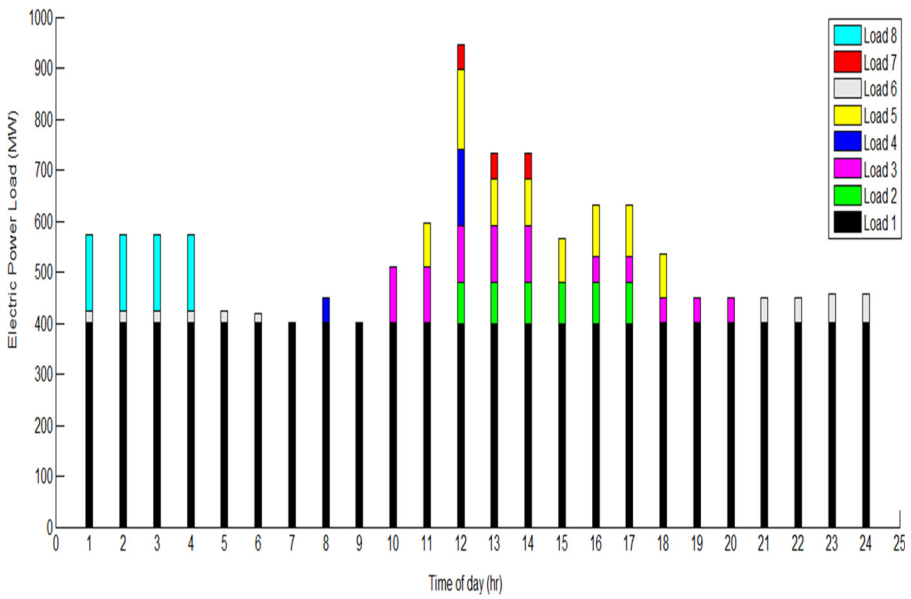

FIG. 8. Commercial customers' optimal load for energy hub 2.

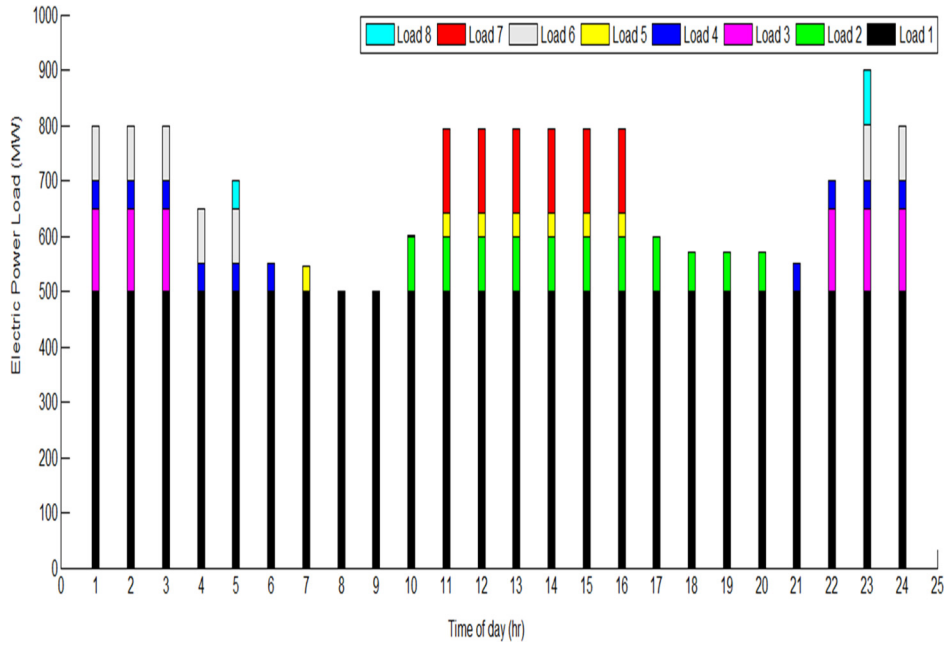

FIG. 9. Industrial customers' optimal load for energy hub 3.

Figures 7–9 show the actual allocation of time for the individual energy hub loads. By scheduling the sequential time shiftable energy hub loads at their best times of operation and adjusting the power shiftable energy hub loads to their best level of operation, the total electricity cost of the energy hub customers was reduced according to their respective time varying electricity tariff pricing structure.

D. Case 2: Effect of energy hub coordination

1. Scenario 1: Distributed control scheme without communication of energy hubs

In this case, the energy hubs are optimized individually, and there is no sharing of excess energy from each energy hub.

a. Energy hub 1: Residential customers. The electricity pricing vector for the residential customers is used in Eq. (30). The output optimal energy hub load is then used to optimise the generation cost and the amount of emission using Eq. (31). The power and heat demand balance for the energy hub is given by

$$L_{ET,t} = C_{TR} * G_{ei,t} + \quad C_{PV} * G_{PV1,t}\,. \tag{34}$$

Figure 10 shows the optimal power generation distribution for thermal power generations connected at energy hub 1. The three thermal power generations are evenly distributed at each respective time of the day.

b. Energy hub 2: Commercial customers. Similarly, the electricity pricing vector for the commercial customers is used in Eq. (30), and the output optimal energy hub load becomes the input to Eq. (31). The power and heat demand balance for the energy hub is given as follows:

$$\begin{bmatrix} L_{ET,t} \\ L_{HT,t} \end{bmatrix} = \begin{bmatrix} C_{TR} & C_{PV2} & C_{ngE} \\ 0 & 0 & C_{ngH} \end{bmatrix} \begin{bmatrix} G_{e,t} \\ G_{PV2,t} \\ G_{ng,t} \end{bmatrix}. \tag{35}$$

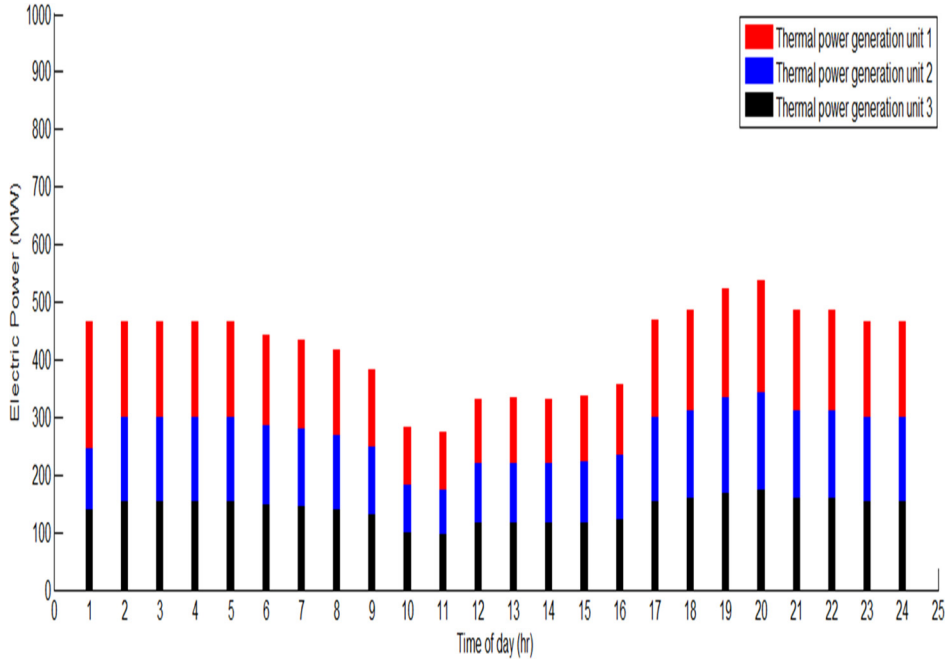

FIG. 10. Optimal power generation output for thermal generation units at energy hub 1.

Figure 11 shows the optimal power distribution for power generation units connected at energy hub 2. It can be clearly seen that the CHP unit always operates at maximum at all the times of the day, and thus, the maximum efficient use of clean energy is achieved.

c. Energy hub 3: Industrial customers. The electricity pricing vector for the industrial customers is used in Eq. (30). The output optimal energy hub load is then used in Eq. (31) to optimise the generation cost and the amount of emission for the energy hub. The power and heat demand balance for the energy hub is given as follows:

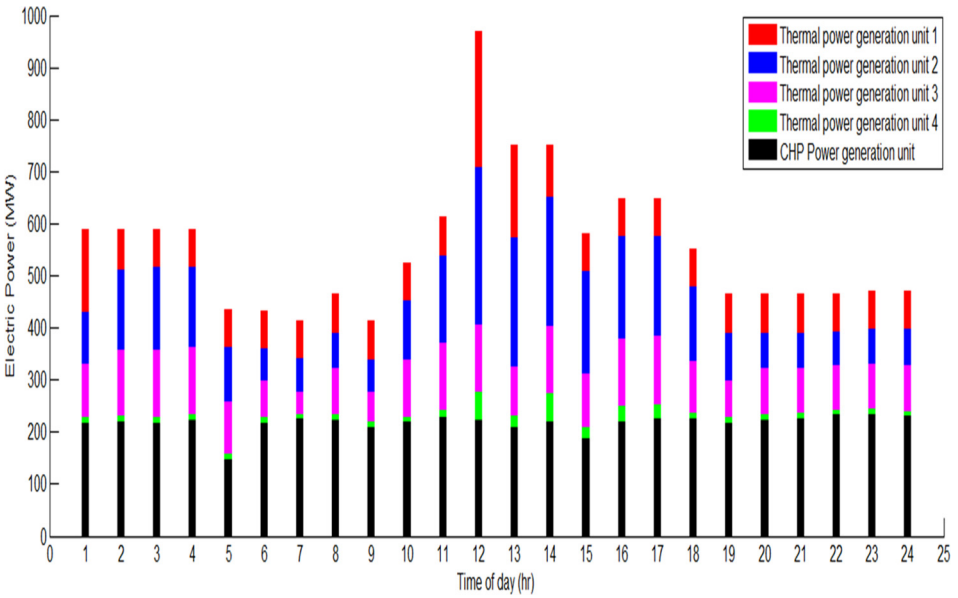

FIG. 11. Optimal power generation output for thermal generation units at energy hub 2.

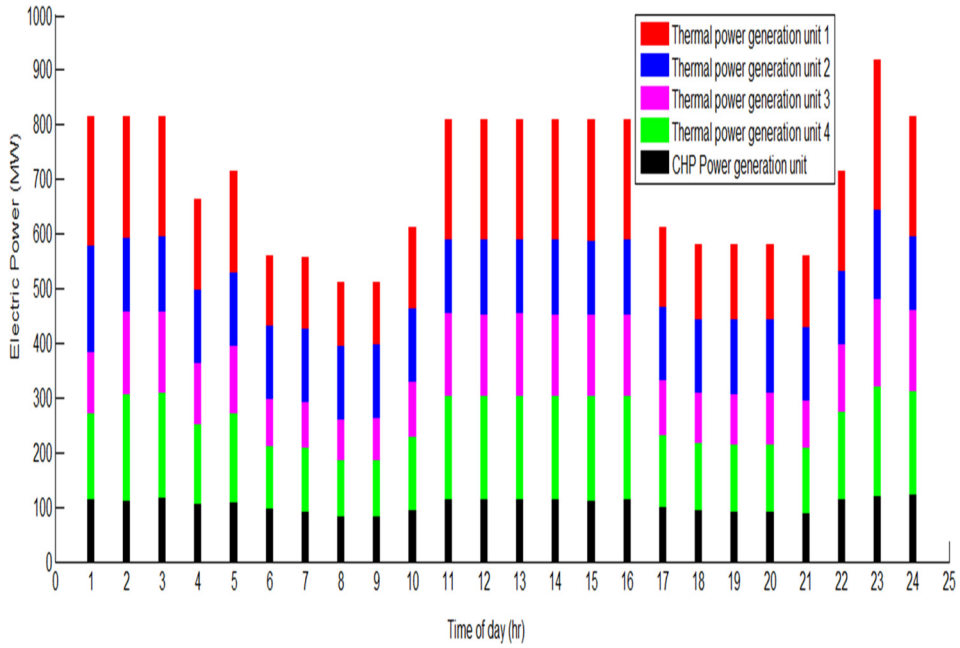

FIG. 12. Optimal power generation output for thermal generation units at energy hub 3.

$$\begin{bmatrix} L_{ET,t} \\ L_{HT,t} \end{bmatrix} = \begin{bmatrix} C_{TR} & C_{ngE} \\ 0 & C_{ngH} \end{bmatrix} \begin{bmatrix} G_{e,t} \\ G_{ng,t} \end{bmatrix}, \tag{36}$$

Figure 12 shows the optimal power distribution for power generation units connected at energy hub 3. The maximum power generation is achieved between 11:00 h–16:00 h and 23:00 h–03:00 h.

2. Scenario 2: Centralised control scheme: DR-DEED modelling

In a centralised energy hub system network, the central supervisory controller receives the initial objective energy hub load profile and electricity pricing as inputs from different energy hubs. Then, it sets the required load control actions to minimize the respective hub customers' electricity cost using Eq. (30). The output load profile is used as an input to the DEED optimisation problem and is solved using Eq. (31). The power and heat demand balance constraints used in these analyses are explained below.

a. Power and heat demand balance constraints. From the case study, the converter efficiency data for each converter is similar, i.e., $C_{TR1} = C_{TR2} = C_{TR3}$, $C_{PV1} = C_{PV2}$, and $C_{NG1} = C_{NG2}$. The total power and heat demand balance for the whole system network is therefore given by Eqs. (37) and (38). Table X shows the actual power distribution of all the power generation units connected to the multi-energy hub system network for the whole day. At all times of the day, it can be clearly seen that the CHP units are operational. The CHP unit connected at Energy Hub 1 (CHP1) attains its maximum power generation at 19:00 h, while the CHP unit connected at Energy Hub 2 (CHP2) attains its maximum power generation at 06:00 h and 00:00 h

$$L_{ET,t} = C_{TR} \sum_{i=1}^{N} P_i^t + C_{ngE} \sum_{j=1}^{Z} P_{nge,j}^t + C_{PV} \sum_{k=1}^{Y} P_{PV,k}^t \quad \forall t \in T, \tag{37}$$

$$L_{HT,t} = C_{ngH} \sum_{j=1}^{Z} G_{ngH,j}^t \quad \forall t \in T, \tag{38}$$

TABLE X. Optimal power output for thermal power generation units and CHP generation units of the multi-energy hub system network.

		Time (h)											
	Gen. No.	1	2	3	4	5	6	7	8	9	10	11	12
Hub 1	1	220.00	167.06	159.96	136.98	121.65	100.00	100.00	100.00	100.00	100.00	132.43	199.04
	2	107.48	146.39	140.59	121.79	109.27	86.81	81.19	79.07	63.93	85.38	118.08	172.53
	3	140.00	153.07	148.05	131.80	120.97	101.55	96.69	94.85	81.76	100.31	128.59	175.67
Hub 2	1	160.00	80.00	73.00	73.00	73.00	73.00	73.00	73.00	73.00	73.00	73.00	73.00
	2	190.00	240.00	285.46	253.89	232.85	195.13	185.69	182.13	156.70	192.72	247.65	300.00
	3	110.00	130.00	130.00	130.00	130.00	130.00	130.00	130.00	130.00	130.00	130.00	130.00
	4	47.74	55.00	55.00	55.00	49.28	29.86	25.00	23.17	10.08	28.62	55.00	55.00
	CHP 1	218.20	219.98	218.02	222.11	224.78	219.80	224.07	223.36	222.82	218.56	227.27	221.22
Hub 3	1	220.00	167.06	159.96	136.97	121.65	100.00	100.00	100.00	100.00	100.00	132.43	199.04
	2	107.48	146.39	140.59	121.79	109.27	86.81	81.19	79.07	63.93	85.38	118.08	172.525
	3	160.00	145.67	140.66	135.00	135.00	135.00	135.00	135.00	135.00	135.00	135.00	168.27
	4	78.07	111.72	106.70	90.44	79.61	60.19	57.00	57.00	57.00	58.95	87.23	134.32
	CHP 2	111.80	110.74	115.13	111.05	110.44	121.17	117.24	115.28	113.77	113.31	112.56	112.11
	Gen. No.	13	14	15	16	17	18	19	20	21	22	23	24
Hub 1	1	163.79	163.03	139.11	152.17	138.21	121.51	113.28	116.69	106.16	126.31	154.76	139.43
	2	143.72	143.09	123.54	134.22	122.81	109.16	102.43	105.21	96.61	113.08	136.34	123.81
	3	150.76	150.22	133.31	142.54	132.68	120.87	115.05	117.46	110.02	124.26	144.38	133.54
Hub 2	1	73.00	73.00	73.00	73.00	73.00	73.00	73.00	73.00	73.00	73.00	73.00	73.00
	2	290.72	289.67	256.83	274.76	255.60	232.67	221.36	226.04	211.59	239.25	278.32	257.27
	3	130.00	130.00	130.00	130.00	130.00	130.00	130.00	130.00	130.00	130.00	130.00	130.00
	4	55.00	55.00	55.00	55.00	55.00	49.19	43.37	45.78	38.34	52.58	55.00	55.00
	CHP 1	215.36	220.16	218.02	220.33	225.49	225.49	234.73	223.53	225.13	232.07	233.67	229.22
Hub 3	1	163.79	163.03	139.11	152.17	138.21	121.51	113.28	116.69	106.16	126.31	154.76	139.43
	2	143.72	143.09	123.54	134.22	122.81	109.16	102.43	105.21	96.61	113.08	136.34	123.81
	3	143.36	142.82	135.00	135.15	135.00	135.00	135.00	135.00	135.00	135.00	136.98	135.00
	4	109.41	108.87	91.96	101.19	91.33	79.52	73.70	76.11	68.67	82.91	103.02	92.19
	CHP 2	112.71	111.80	111.65	111.80	111.50	115.28	113.31	114.22	115.28	118.00	119.36	121.63

where N, Z, and Y are the total number of thermal power generation units, CHP power generation units, and solar PV power generation units in the energy hub network, respectively. P_i^t is the electric power generation by the ith thermal power generation unit at any given time t, $P_{nge,j}^t$ is the electric power by the jth CHP unit at any given time t, $G_{ngH,j}^t$ is the heat generation by the jth CHP unit at any given time t, and $P_{PV,k}^t$ is the electric power generation by the kth solar PV power generation unit at any given time t.

3. Distributed control scheme with communication: Scenario 3–scenario 8

In this case, all the scenarios are solved in the same fashion. Each energy hub is able to communicate with neighbouring energy hubs in order to balance its power and heat demand. Excess energy from each energy hub is shared among neighbouring energy hubs. The exchange of information between the energy hubs enables the minimization of generation cost, the amount of emission, and electricity cost in all the energy hubs. There are six possible ways of communication between the three energy hubs. Each possible way of communication was considered as a scenario. DR-DEED optimisation was applied to all the possible scenarios, and

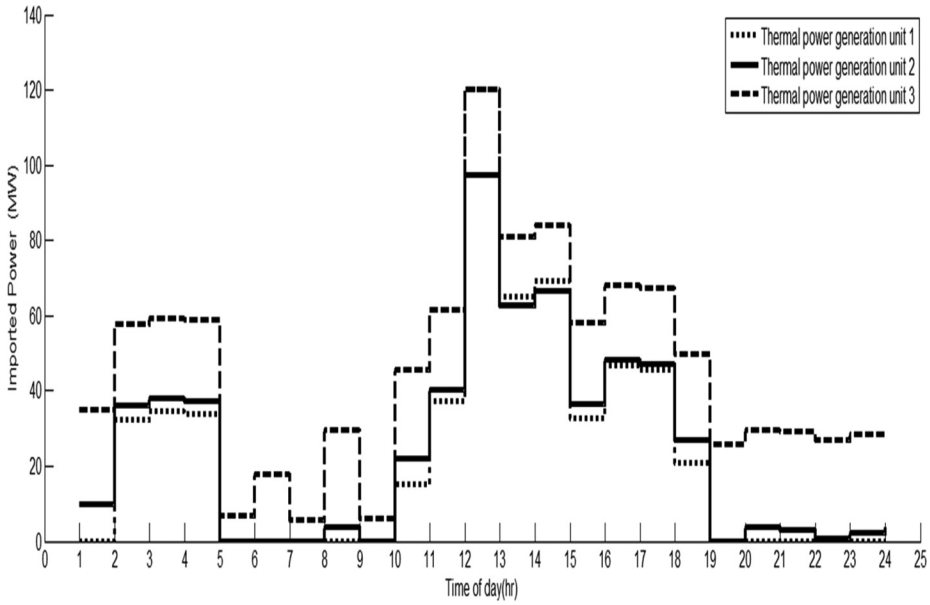

FIG. 13. Optimal power import for thermal generation units for scenario 3 between energy hub 1 to energy hub 2.

comparisons were done in terms of the optimal power import by energy hubs, generation cost, and the amount of emission (see Figures 13–24). The formulation of the problem uses equations that are derived from the individual energy hub optimisation problems of scenario 1. However, virtual power plants are used to represent excess energy from each energy hub, which may be passed on to the next energy hub depending on the possible combination followed. The DR-DEED optimisation for each scenario has the following steps:

- *Step 1:* Solve the DR optimisation model for the energy hub under consideration as in scenario 1.
- *Step 2:* The output load from the energy hub is used to perform DEED optimisation for the respective energy hub.

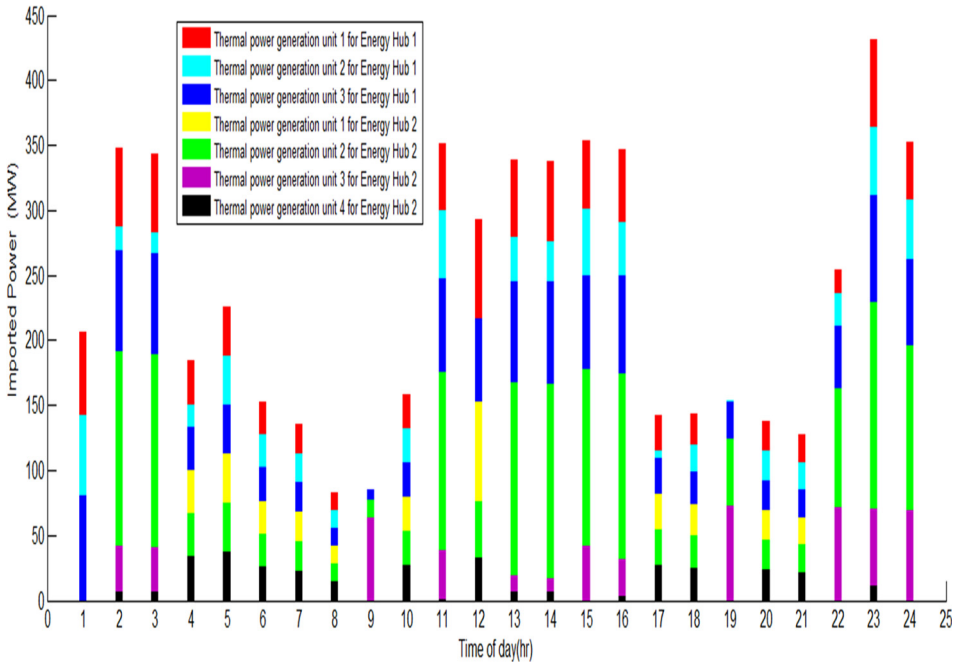

FIG. 14. Optimal power import for thermal generation units for scenario 3 between energy hubs 1 and 2 and energy hub 3.

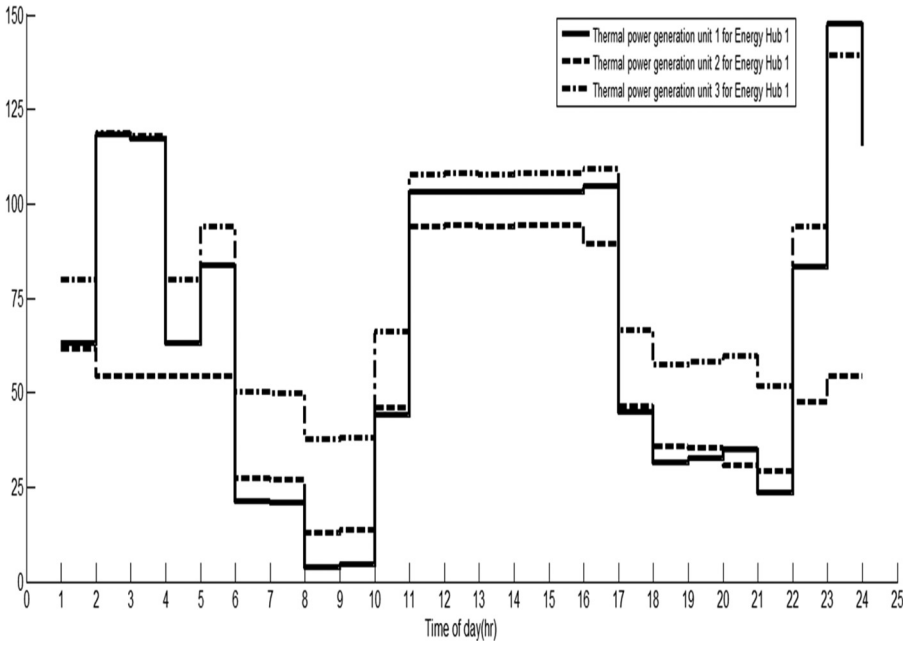

FIG. 15. Optimal power import for thermal generation units for Scenario 4 between energy hub 1 and energy hub 3.

- *Step 3:* Calculate the excess energy for the energy hub.
- *Step 4:* The excess energy from the respective energy hub is used as a virtual power plant in the corresponding energy hub that is being fed.
- *Step 5:* Repeat *step 1–step 4* for the next energy hub including the virtual power plant (i.e., excess energy from the first energy hub) to balance the power and heat demand of the respective energy hub.
- *Step 6:* Repeat *step 1–step 4* for the third energy hub including the virtual power plant (i.e., excess energy from the first and second energy hubs) to balance the power and heat demand of the respective energy hub.

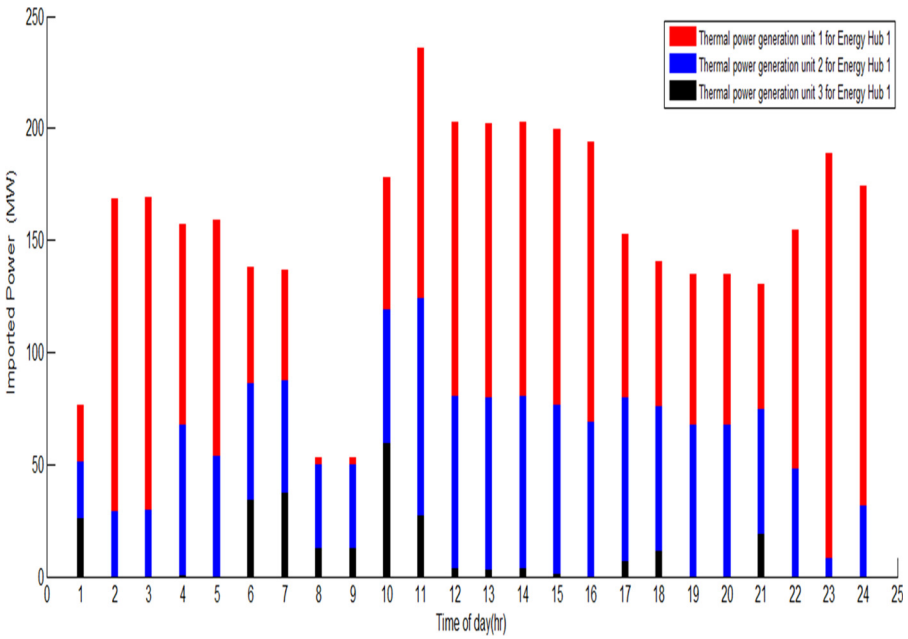

FIG. 16. Optimal power import for thermal generation units for scenario 4 between energy hubs 1 and 3 and energy hub 2.

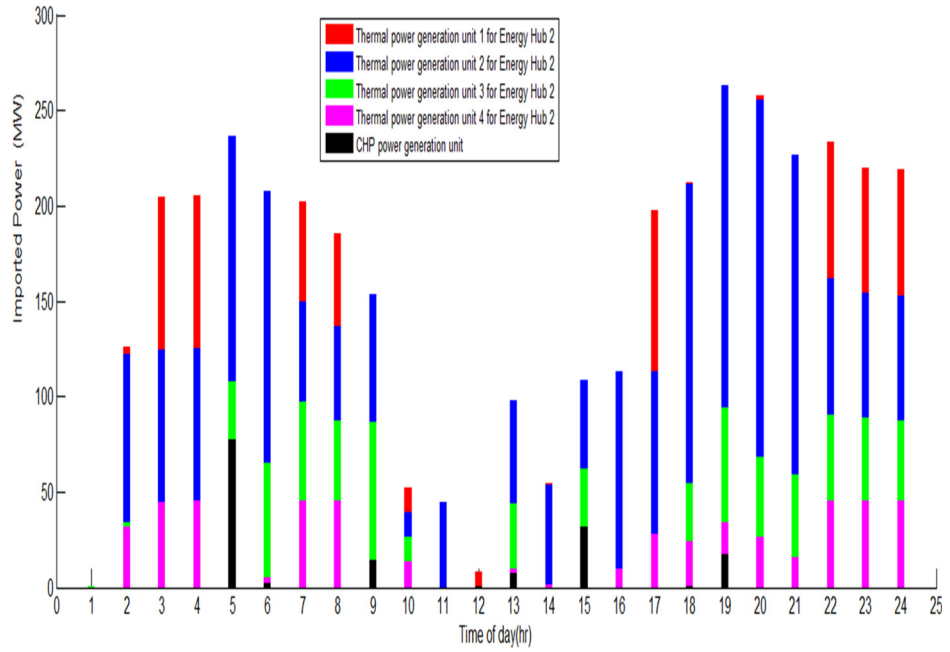

FIG. 17. Optimal power import for thermal generation units for scenario 5 between energy hub 2 and energy hub 1.

IV. DISCUSSION OF RESULTS

Figure 25 shows the amount of emission from generation units for all the scenarios considered in case 2. Generally, the weighting factor μ affects the amount of emission from all generation units for all the scenarios considered. On average, the lowest amount of emission is achieved when scenario 5 is employed. Giving more emphasis to the amount of emission of generation units, i.e., $\mu = 0$, the centralised control scheme has the highest amount of emission, while scenario 5 has the lowest. In general, it can also be clearly seen from the figure that as

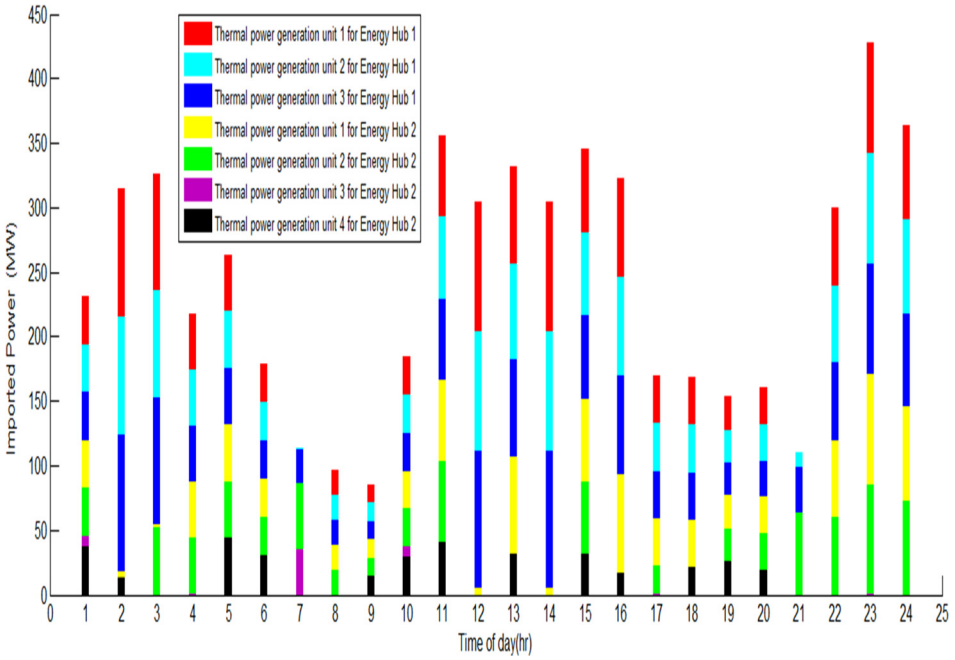

FIG. 18. Optimal power import for thermal generation units for scenario 5 between energy hubs 2 and 1 and energy hub 3.

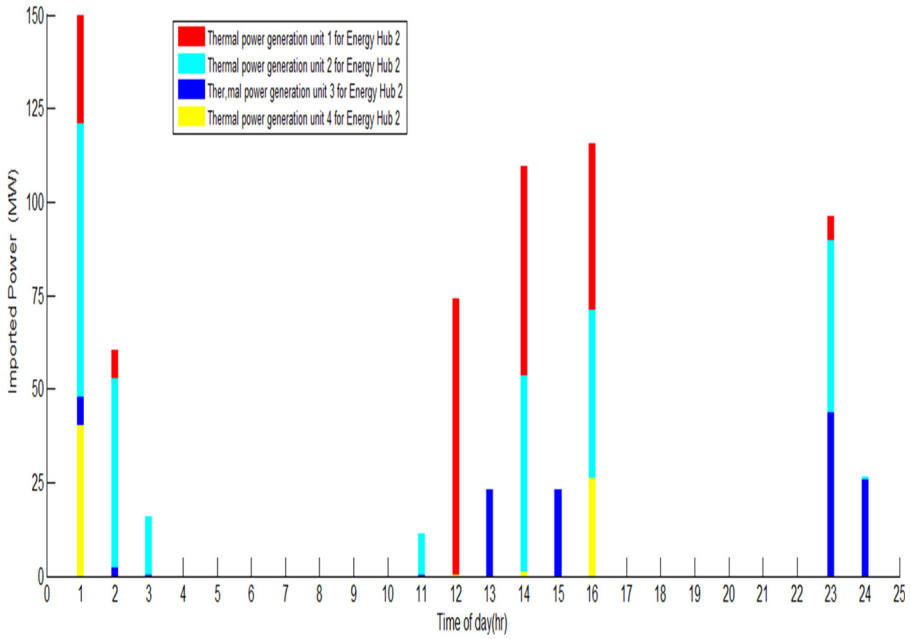

FIG. 19. Optimal power import for thermal generation units for scenario 6 between energy hub 2 and energy hub 3.

the value of μ increases, the amount of emission also increases with the exception of scenario 4. There is a sharp increase of $\approx 250\%$ in the amount of emission when μ is increased between 0 and 0.5 for scenario 6. In scenario 4, a reduction of less than 10% in the amount of emission is achieved when μ is increased from 0.5 to 1. For all the scenarios, the highest amount of emission is achieved in scenario 6 when μ is set at either 0.5 or 1. Scenarios 1 and 2 are almost similar for all values of μ. Scenario 2 has a higher amount of emission for all values of μ when compared to scenarios 3, 4, and 5. The results therefore clearly show that when different energy hubs are integrated together, the amount of emission can be greatly reduced.

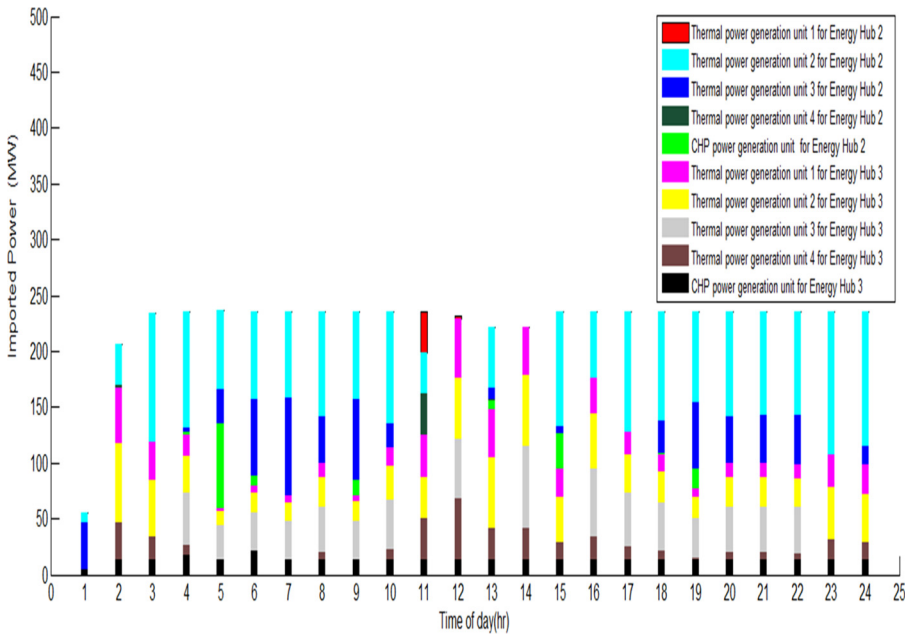

FIG. 20. Optimal power import for thermal generation units for scenario 6 between energy hubs 2 and 3 and energy hub 1.

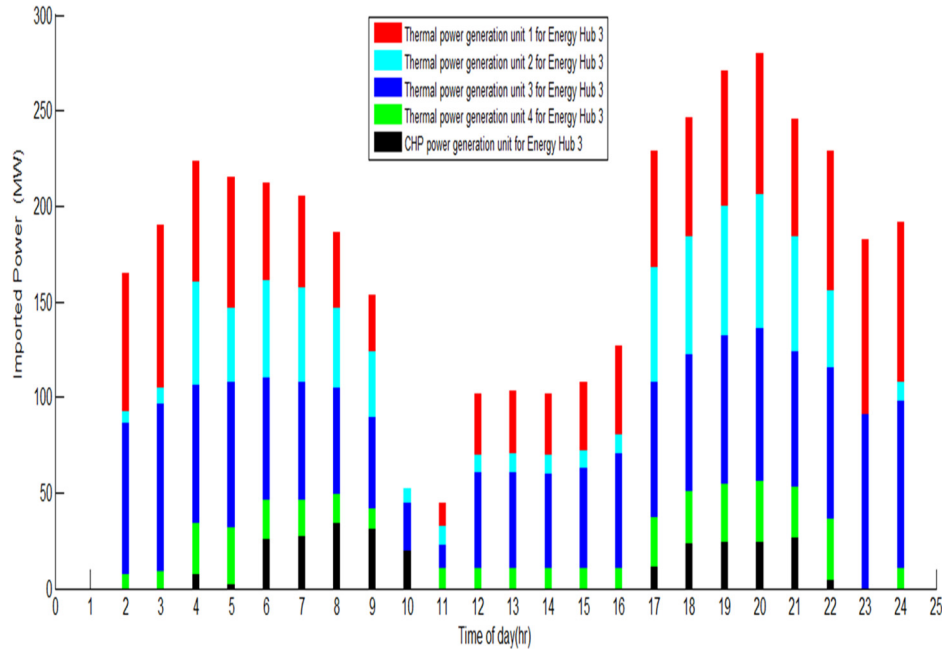

FIG. 21. Optimal power import for thermal generation units for scenario 7 between energy hub 3 and energy hub 1.

In the case of generation cost, i.e., Fig. 26, the value of the weighting factor μ does not affect the generation cost. However, the coordination of the energy hubs has a great effect on the generation cost. The lowest generation cost is achieved when scenario 1, i.e., distributed control scheme without communication, is employed. Scenarios 4, 6, 7, and 8 also generally have low generation costs. The highest generation costs are achieved in scenarios 2, 3, and 5. The generation costs decrease by more than 50% in scenarios 1, 4, 6, 7, and 8 with respect to scenarios 2, 3, and 5. It can also be clearly seen that it is difficult to have a set of control

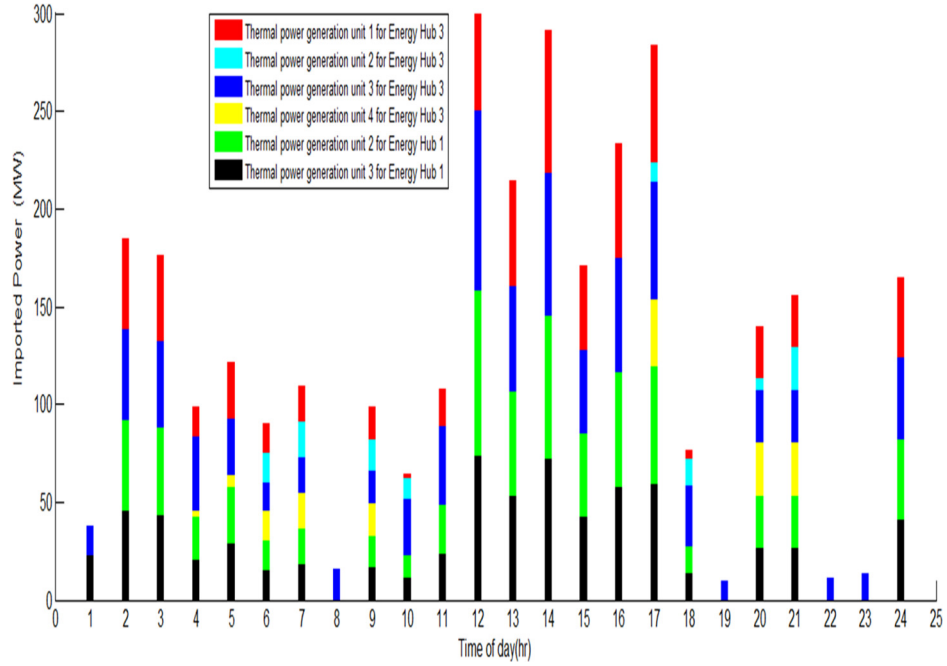

FIG. 22. Optimal power import for thermal generation units for scenario 7 between energy hubs 3 and 1 and energy hub 2.

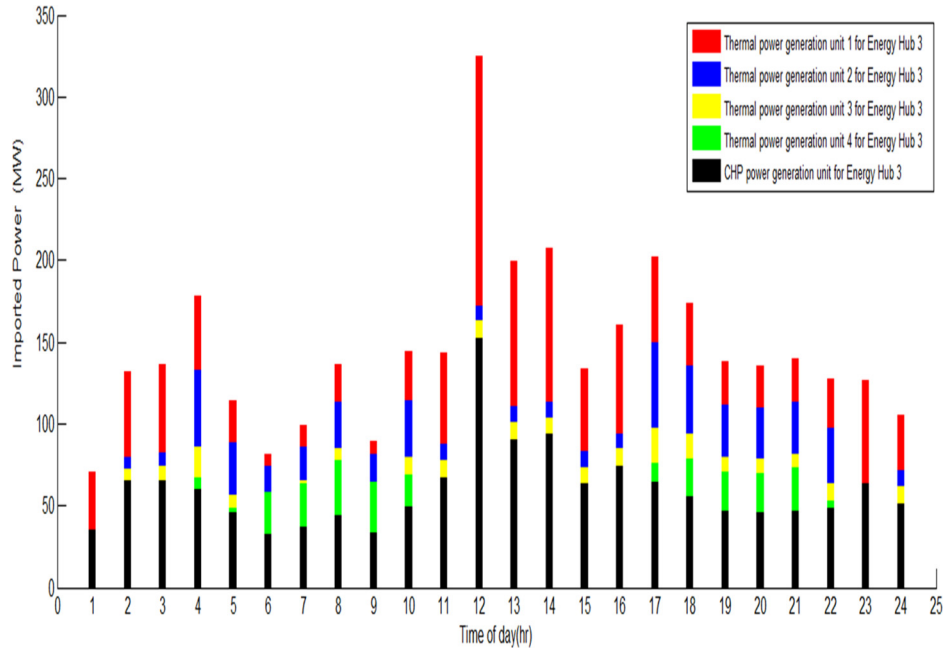

FIG. 23. Optimal power import for thermal generation units for scenario 8 between energy hub 3 and energy hub 2.

schemes that give both the low amount of emission and generation costs at the same time. For scenarios 2, 3, and 5, putting more emphasis on the emission, i.e., the decreasing weighting factor μ, results in higher cost of power generation and less pollution, whereas putting more emphasis on generation cost or the increasing weighting factor (μ), a high amount of emission is generated at lower generation cost for scenarios 1, 6, 7, and 8. When there is a balance between the amount of emission and the generation costs, i.e., $\mu = 0.5$, the conditions generally favour distributed control strategies, (i.e., Scenarios 4, 7, and 8), demonstrating the benefits of

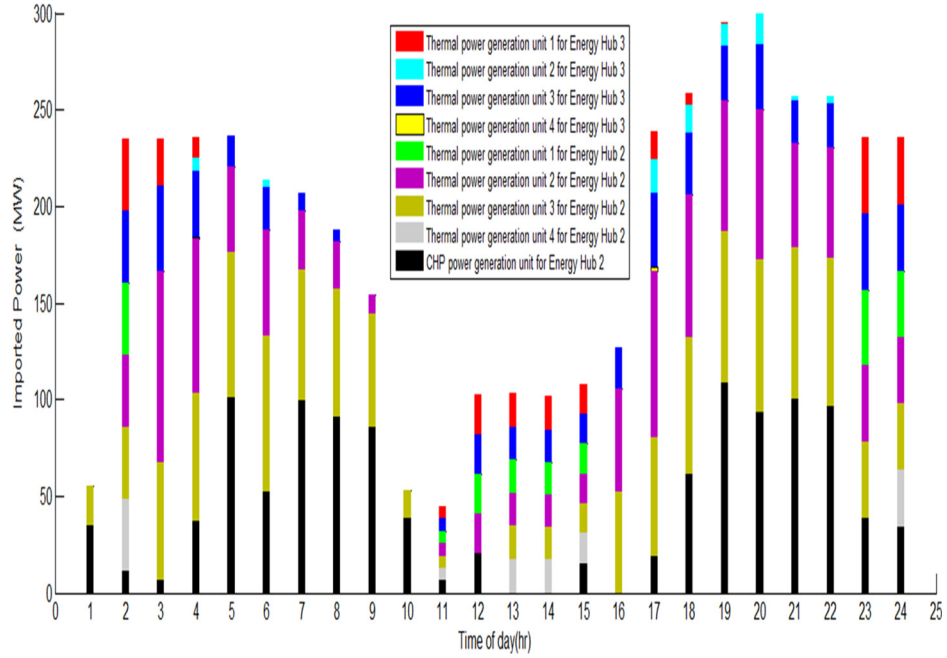

FIG. 24. Optimal power import for thermal generation units for scenario 8 between energy hubs 3 and 2 and energy hub 1.

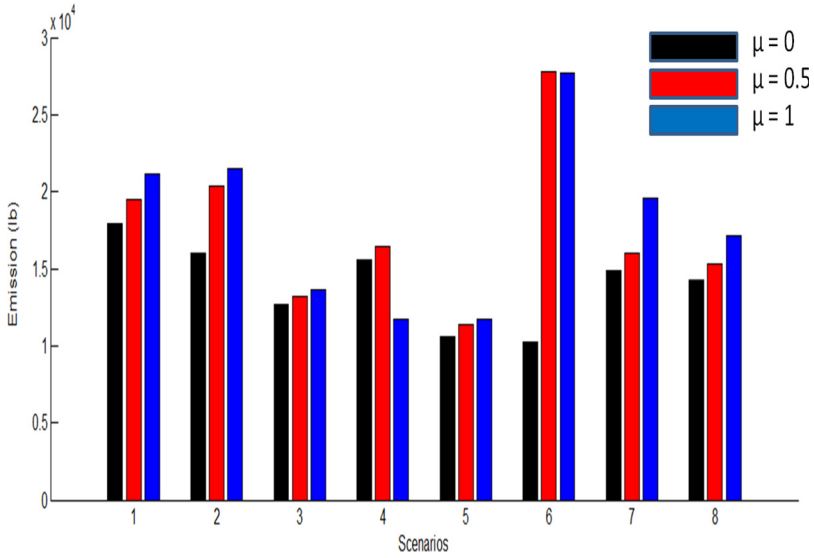

FIG. 25. Amount of emission from thermal power generation units for all scenarios.

networking between energy hubs. Therefore, there is a need for a trade-off between generation costs and the amount of emission when distributed control schemes are employed for different sparsely located distributed energy hubs.

The value of power import from each energy hub was calculated with $\mu = 0.5$. Generally, there are similarities in all the scenarios in terms of the power import profile from neighbouring energy hubs. The lowest power import is experienced in scenario 6 between energy hubs 2 and 3. For most part of the day, there is no import of power from energy hub 2. The maximum import of power is experienced at 01:00 h. When all energy hubs are treated as standalone, i.e., scenario 1, the power demand from all the thermal power generation units and CHP units generally follows the energy hub load demand profile. For energy hubs 2 and 3, it can be clearly seen that the CHP units of the respective energy hubs provide almost their maximum power generation for all the 24 h considered. The results demonstrate that the maximum use of

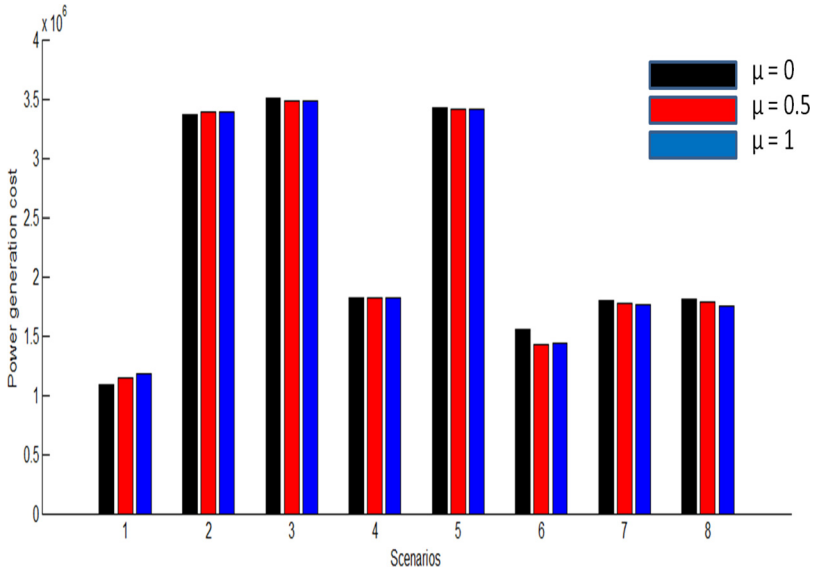

FIG. 26. Generation cost of thermal power generation units for all scenarios.

distributed energy systems such as CHP units is achieved when they participate in an integrated energy hub system network.

In scenario 4, the amount of power imported by energy hub 3 is much higher than that imported by energy hub 2. The reason is that the thermal power generation units at energy hub 3 are too expensive to generate the power for the respective energy hub load. The power generation from CHP units of energy hub 3 is exported to energy hub 1, contributing almost 13% of the total energy demand during the peak hour at 23:00 h. The maximum power import by energy hubs 2 and 3 occurs at 23:00 h and 11:00 h, respectively. No CHP power is exported from energy hub 3 to energy hub 2.

In scenario 7, all thermal power generation units export power to energy hub 2 throughout the whole day. The maximum power export is at 12:00 h, and during this time, the CHP unit of energy hub 3 and thermal power generation unit 1 have maximum power export. It is thus expected as this is the time when there is maximum energy hub load demand for energy hub 2. In the same scenario, power import from energy hub 1 attains a maximum of ≈300 MW at 20:00 h compared to ≈700 MW at 12:00 h for energy hub 2. There is therefore more power import from energy hub 2 than from energy hub 1. The minimum power import for energy hub 1 occurs at 01:00 h and 10:00 h–11:00 h. The CHP unit for energy hub 2 supplies its maximum power to energy hub 1 at 19:00 h–22:00 h and 05:00 h–09:00 h. Therefore, through the interdependency or mutual interactions of the energy hubs, great benefits of sharing power generation between the energy hubs are achieved.

Table X shows optimised power output for thermal power generation units and CHP units of the multi-energy hub system using the centralised control scheme. It is worthwhile to note that both CHP units have their power output approximately following the heat demand. The peak power output demand is ≈234 kW and ≈122 kW for CHP 1 and CHP 2, respectively. The reason for this is that since the power generation of each CHP unit is dependent on its respective heat generation at any particular given time, the energy hub heat demand reaches its peak at these respective hours.

In scenario 8, all generation units at energy hub 3 exported power to energy hub 2. This means that most of the thermal power generation units at hub 3 generate much cheaper power than those at energy hub 2. However, when both energy hubs are able to export to energy hub 1, it can be seen that an average of ≈250 MW is exported to energy hub 1 throughout the whole day with the exception of a minimum of ≈50 MW at 01:00 h. This points out that there is a great advantage of controlling each energy hub and exporting the excess power to the neighbouring energy hubs. The excess energy can be exported using a different tariff strategy as a result of the transmission cost involved. In this paper, however, the export cost of excess energy from each energy hub is not included in the analyses. It should therefore be noted that the use of these other factors may change the results of the case study.

From the analyses of the above results, it can be concluded that the participation of clean distributed energy systems such as CHP in an integrated energy hub system network is important to achieve maximum benefits. The results also show that policy makers, power system planners, and operators have to give priority for balancing emission, power generation costs, and power export capabilities of energy hubs when designing control strategies for different sparsely located distributed energy hubs.

V. CONCLUSION

The case study presented in this paper shows the potential of DR strategies and energy hub coordination. The DR-DEED optimisation model applied in the case study allows for a comparison of more sustainable energy hub control schemes, including the evaluation of economic and environmental criteria and power import between energy hubs. The results show that the weighting factor μ has no significant relationship with the total generation cost of the power generation units in the energy hubs for all scenarios considered. However, a significant reduction of generation cost is achieved when different control strategies are employed for the energy hubs. The import of power from each energy hub in different scenarios is influenced by the generation cost of the

energy hubs that are involved. Thermal power generation units with less generation cost export more excess power to neighbouring energy hubs than those that are costly. The fact that it is difficult to have a set of distributed control schemes that give both low amounts of emission and generation costs at the same time points to the need to accurately assess the generation cost and the amount of emission for all energy sources to come up with accurate multi-energy hub system management frameworks that are sustainable and environmentally friendly.

The contribution of this paper focuses on redesigning of the power system network as the number of geographically dispersed energy hub systems integrated to the conventional power system network continues to increase. Future research work will focus on investigating the influence of different levels of centralised and integrated technologies on the operation and optimisation of this smart multi-energy hub system network. In addition, the participation of neighbouring energy hubs in the electricity price market is an additional research area to be explored. The developed control strategy will be applied to larger integrated energy system networks with more than three interconnected energy hubs.

[1]S. Perry, J. Kleme, and I. Bulatov, "Integrating waste and renewable energy to reduce the carbon footprint of locally integrated energy sectors," Energy **33**(10), 1489–1497 (2008).
[2]M. Akorede, H. Hizam, and E. Rouresmaeil, "Distributed energy resources and benefits to the environment," Renewable Sustainable Energy Rev. **14**, 724–734 (2010).
[3]H. Farhangi, "A road map to integration: Perspectives on smart grid development," IEEE Power Energy Mag. **12**(3), 52–66 (2014).
[4]P. Mancarella, "MES (multi-energy systems): An overview of concepts and evaluation models," Energy **65**, 1–17 (2014).
[5]O. Kristina, R. Evins, and V. Dorer, "Integration of decentralized energy systems in neighbourhoods using the energy hub approach," Appl. Energy **154**, 277–289 (2015).
[6]M. Geidl, G. Koeppel, P. Favre-Perrod, B. Klockl, G. Andresson, and K. Frolich, "Energy hubs for the future," IEEE Power Energy Mag. **5**(1), 24–30 (2007).
[7]G. Chicco and P. Mancarella, "Distributed multi-generation: A comprehensive view," Renewable Sustainable Energy Rev. **13**(3), 535–551 (2009).
[8]H. Ren and W. Gao, "A MILP model for integrated plan and evaluation of distributed energy systems," Appl. Energy **87**(3), 1001–1014 (2010).
[9]C. Weber and N. Shah, "Optimisation based design of a district energy system for an eco-town in the United Kingdom," Energy **36**(2), 1292–1308 (2011).
[10]ICF International, "The future of natural gas in Mozambique: Towards a natural gas master plan," Consultant report for World Bank and Government of Mozambique, Report No. 80683, 2012.
[11]I. Gqada, "Mozambiques gas: An opportunity for South Africa?," in *SAIIA: Governance of Africa's Resources Programme: Policy Briefing 53* (2012), pp. 1–3.
[12]A. Omu, R. Choudhary, and A. Boies, "Distributed energy resource system optimisation using mixed integer linear programming," Energy Policy **61**, 249–266 (2013).
[13]M. Nazar and M. Haghifam, "Multiobjective electric distribution system expansion planning using hybrid energy hub concept., Electrical," Power Syst. Res. **79**(6), 899–911 (2009).
[14]A. Manijeh, K. Zare, and B. Mohammadi-Ivatloo, "Short-term scheduling of combined heat and power generation units in the presence of demand response programs," Energy **71**, 289–301 (2014).
[15]M. Arnold, R. Negenborn, G. Andersson, and B. De Schutter, "Intelligent infrastructure," in *Distributed Predictive Control for Energy Hub Coordination in Coupled Electricity and Gas Networks*, Intelligent Systems, Control Automation: Science Engineering (Springer, 2010), Vol. 42, pp. 235–273.
[16]J. Yoona, R. Bladicka, and A. Novoselac, "Demand response for residential buildings based on dynamic price of electricity," Energy Build. **80**, 531541 (2014).
[17]R. Evins, K. Orehounig, V. Dorer, and J. Carmeliet, "New formulations of the energy hub model to address operational constraints," Energy **73**, 387–398 (2014).
[18]A. Parisio, V. Carmen Del, and A. Vaccaro, "A robust optimization approach to energy hub management," Int. J. Electr. Power Energy Syst. **42**(1), 98–104 (2012).
[19]M. Schulze, L. Friedrich, and M. Gautschi, "Modeling and optimization of renewables: applying the energy hub approach," in IEEE International Conference on Sustainable Energy Technologies (ICSET) (2008).
[20]J. Keirstead, M. Jennings, and A. Sivakumar, "A review of urban energy system models: Approaches, challenges and opportunities," Renewable Sustainable Energy Rev. **16**, 3847–3866 (2012).
[21]A. J. Conejo, J. M. Morales, and L. Baringo, "Real-time demand response model," IEEE Trans. Smart Grid **3**(3), 236–242 (2010).
[22]S. An, Q. Li, and T. W. Gedra, "Natural gas and electricity optimal power flow," in *IEEE PES Transmission and Distribution Conference* (2003), pp. 138–143.
[23]A. M. Elaiw, A. M. Shehata, and M. A. Alghamdi, "A model predictive control approach to combined heat and power dynamic economic dispatch problem," Arab J. Sci. Eng. **39**, 7117–7125 (2014).
[24]N. Nwulu and X. Xia, "Multi-objective dynamic economic emission dispatch of electric power generation integrated with game theory based demand response programs," Energy Convers. Manage. **89**, 963–974 (2015).